

**Original scientific paper**

**TEMPERATURE-DEPENDENT PHYSICAL CHARACTERISTICS  
OF THE ROTATING NONLOCAL NANOBELMS SUBJECT TO A  
VARYING HEAT SOURCE AND A DYNAMIC LOAD**

**Ahmed E. Abouelregal<sup>1,2</sup>, Hamid Mohammad-Sedighi<sup>3,4</sup>,  
Seyed Ali Faghidian<sup>5</sup>, Ali Heidari Shirazi<sup>3</sup>**

<sup>1</sup>Department of Mathematics, College of Science and Arts, Jouf University, Al-Qurayyat,  
Saudi Arabia

<sup>2</sup>Department of Mathematics, Faculty of Science, Mansoura University, Mansoura, Egypt

<sup>3</sup>Mechanical Engineering Department, Faculty of Engineering, Shahid Chamran University  
of Ahvaz, Ahvaz, Iran

<sup>4</sup>Drilling Center of Excellence and Research Center, Shahid Chamran University of Ahvaz,  
Ahvaz, Iran

<sup>5</sup>Department of Mechanical Engineering, Science and Research Branch, Islamic Azad  
University, Tehran, Iran

**Abstract.** *In this article, the influence of thermal conductivity on the dynamics of a rotating nanobeam is established in the context of nonlocal thermoelasticity theory. To this end, the governing equations are derived using generalized heat conduction including phase lags on the basis of the Euler–Bernoulli beam theory. The thermal conductivity of the proposed model linearly changes with temperature and the considered nanobeam is excited with a variable harmonic heat source and exposed to a time-dependent load with exponential decay. The analytic solutions for bending moment, deflection and temperature of rotating nonlocal nanobeams are achieved by means of the Laplace transform procedure. A qualitative study is conducted to justify the soundness of the present analysis while the impact of nonlocal parameter and varying heat source are discussed in detail. It also shows the way in which the variations of physical properties due to temperature changes affect the static and dynamic behavior of rotating nanobeams. It is found that the physical fields strongly depend on the nonlocal parameter, the change of the thermal conductivity, rotation speed and the mechanical loads and, therefore, it is not possible to neglect their effects on the manufacturing process of precise/intelligent machines and devices.*

**Key words:** *Nonlocal Elasticity, Rotating Nanobeam, Thermoelasticity, Variable Thermal Conductivity, Varying Load*

---

Received December 22, 2020 / Accepted February 28, 2021

**Corresponding author:** Hamid Mohammad-Sedighi

Mechanical Engineering Department, Faculty of Engineering, Shahid Chamran University of Ahvaz, Ahvaz, Iran

E-mails: [h.msedighi@scu.ac.ir](mailto:h.msedighi@scu.ac.ir); [hmsedighi@gmail.com](mailto:hmsedighi@gmail.com)

## 1. INTRODUCTION

Thermomechanical effects resulting from the interaction of temperature and deformation fields are of particular significance in various modern designs such as high-speed aircrafts, jets, gas and steam turbines, nuclear reactors and missiles. Both theoretical and practical concerns, including a rapid supply of thermal energy, have been gaining increasing attention. The conventional heat conduction theory, on the basis of the Fourier's law, takes an instant reaction to the temperature gradient and gives a distinctive parabolic equation for temperature change.

To solve the infinite speed thermal propagation phenomena predicted by the classical thermoelasticity theory, modified generalized theories of thermoelasticity have been established. Lord and Shulman [1] suggested one of the modified generalized thermoelasticity theories containing a relaxation time by introducing a novel rule for thermal conductivity to modify the classic Fourier law. The refined law includes the heat flux and its partial derivative with respect to time. Among the models that have gained great popularity in recent years, the model presented by Tzou [2-4] is of great interest to the researchers in the field. In this model, Tzou introduced thermal heat conduction model with dual-phase lag (DPL) to include the effects of microscopic reactions in the rapid transit of heat transfer mechanism into a microscopic formula. In the constitutive relationship between the temperature gradient and heat flux, two different phase-lags have been introduced. Many efforts were made to overcome the problem of unlimited speeds of heat waves predicted by the classical thermoelasticity theory [5-8].

At high operating temperatures, thermal conductivity becomes more significant in popular areas such as materials science, electronics and building insulation. Temperature has a distinctive impact on thermal conductivity of metals and non-metal materials. Thermal conductivity in physics is defined as the capacity of materials for heat transfer. This specifically occurs in the Fourier's heat conduction theory. It was demonstrated through practical experiments that as temperature rises, thermal conductivity of pure metals decreases. In alloys, any rise in temperature results in increasing thermal conductivity, and generally, the variation of electrical conductivity is smaller than that for temperature [9].

The rapid development in micro-electromechanical systems (MEMS) led to more complex sensors and electronic devices. In order to satisfy the industrial requirements, new technologies have been exploited to design high-tech MEMS products. MEMS structures include mechanical components, e.g. small cantilevers, extensions and films that have been frequently filled with a variety of geometrical measurements and arrangements [10]. The influences of small-scale interactions between the neighboring material particles or constituents must be taken into account for these micro/nano-structures. This effect can be observed in miniaturized sub-micron systems like nano-actuators and nano-sensors, microscopes and micro/nano-electronic systems. It is important for designers and engineers to discover the accurate thermomechanical features of ultra-high sensitive devices in order to attain the true aim of providing for the measure of diversion from associated loads in order to forestall cracks, improve the execution and produce the suitable lifetime for MEMS devices [11].

From the discussion above, the principle of vibration is well-known and well-studied in dual beam systems. Nevertheless, the scale-dependent vibration of beam systems makes few contributions. The structures of scale-dependent nanobeams are constructed from nano-materials with special properties because of their dimensions at the nanoscale.

Nanoparticles, nanowires and nanotubes are common examples of the materials with attractive features in sub-micron scales [12].

Nanomaterials are the base choices of technological products for the next century and have intensified the interest of the scientific community in advanced physics, chemistry, biomedicine and different branches of technological sciences. From mechanical point of view, due to their sub-micron dimensions, the impact of small-scale exhibits significant features resulting from the measurements of atomic fission. The strength of the mechanical piezomagnetic nanosized sensors was studied in post-buckling state by Malikan et al. [13]. A powerful flexomagnetic characteristic is also considered in this research. Furthermore, as a result of the flexomagnetic effects, the stability of the Euler-Bernoulli porous nanobeam was thoroughly investigated by Malikan et al. [14]. The magnetization with strain gradients is related to the flexomagnetism. Malikan et al. [15] created an Euler-Bernoulli beam model incorporating the combination of piezomagnetic-flexomagnetic properties and small-scale effects. Flexoelectricity was also studied for a piezoelectric nanobeam by considering the internal viscoelasticity [16].

As mentioned earlier, the size effect has a great contribution in the static and dynamic behavior of micro and nanoscale structures and should not be neglected, that is, the classical continuum mechanics at nanoscale does not make any sense and must be modified accordingly. Nanomaterials are used in complex nanoelectromechanical systems (NEMS) as well as nanocomposites due to their attractive properties. Nanoscale devices are referred to the structures and systems constructed from nanosize materials. The small-scale impact in the nonlocal elasticity is defined by the assumption that stress vector is related to the entire strain field of the whole body (Eringen, [17]). It is distinct from the classical theory of elasticity. Nonlocal theory takes into account interatomic interactions over a long time and its findings depend on the dimensions of the body. The nonlocal theory includes the knowledge about the long-range forces between points along these lines and the internal length scale is essentially used as a material parameter to detect the small scale effects. Any inconveniences of classical continuum theory can be easily avoided and then on local elasticity theory may appropriately describe the size-dependent phenomena. The use of the conventional theory in studying the behavior of nanostructures is inappropriate in many cases because the classical theories are not responsible for small-scale effects.

Recent nanotechnological considerations have led to the application of nonlocal elasticity in submicron scales and the literature indicates that the nonlocal theory of elasticity is typically used progressively to analyze the nanostructures in a consistent and fair manner. The fundamental contrast of the conventional local elasticity theory to those proposed by Eringen called nonlocal one [17–19] substantially depends on the definition of the stress vector. The nonlocal theory of elasticity, however, has been applied in various fields including elastic wave dispersion, mechanical decomposition, etc.

The Eringen nonlocal elasticity theory (ENET) has been applied in many theoretical investigations on the free vibrations of nanoparticles and nanobeams taking into account the assumptions of Euler-Bernoulli (EBT) and Timoshenko beams (TBT) models [20-27]. Another area of research which is emerging due to its current as well as future applications is therefore theoretical studies on the nanoscale behavior of rotating micro/nanobeams in different environment. Rotating nanostructures include different fields like nano-turbines, nano gears and motors and miniaturized bearings.

Taking into account a great deal of studies on the sustainability of rotating nanoscale structures, this idea is expected to draw significant attention in the future; existing samples

include the analysis of molecular carbon nanotubes and gears, nano-motors and nano-shafts [28, 29]. The dynamics of rotating nanotubes and gears were investigated by Srivastava [30] under a single imposed laser beam. The mathematical modeling for rotating nanomotor was carried out by Lohrasebi and Rafii-Tabar [31]. Nanoelectromechanical (NEMS) devices emerge as the next generation of advanced technology, which is capable of making a significant evolution in people's lives.

Considering that rotating motors and other devices are particularly of interest in advanced technology, nanobeams under rotation are analyzed in the present research to determine their vibrational characteristics. The analysis of vibrational behavior of rotating beam-like structures in the framework of classical theory, thanks to their significance in practical applications, has been an interesting and challenging question in recent decades. Some of these fundamental studies are conducted on homogenous rotating beam structures [32–40].

Research of different features of nanoscale beams is an attractive subject in nanotechnology as it encompasses the electronic and optical characteristics of nano-devices. The main objective of this article is to discover the vibrational behavior of rotating isotropic nanobeams in a mathematical framework using the Eringen's nonlocal theory of elasticity. Since the rotating devices such as rotary engines are of particular importance to such modern technologies, the vibration characteristics of rotating nanobeams are investigated in the current research work. The considered model is on the basis of the Euler-Bernoulli theory, generalized dual phase-lag heat conduction and includes the Coriolis and spin-smoothing phenomena. For the first time ever, the features of the mentioned advanced nano-rotating mechanism are reported. This study would contribute to a thorough understanding of the dynamics of rotating nanobeams. Different aspects of the studied model including thermomechanical vibration, point load and nonlocal effects are taken into account. Moreover, numerical examples are presented to indicate the impact of several parameters on the deflection, temperature change and bending moment of rotating nanobeams. This study will recognize various requirements for design and production of environmentally sensitive resonator machines.

## 2. NONLOCAL MODEL OF THERMOELASTICITY

Eringen [17] theoretically introduced a fundamental continuum mechanics in the context of nonlocal theory of elasticity to explore the structural issues at micro-scale dimensions. For nano-scale beams, the general governing equations of nonlocal constituent relations can be described as follows [18]

$$[1 - (e_0 a)^2 \nabla^2] \tau_{kl} = \sigma_{kl}, \quad (1)$$

where  $e_0$  denotes a correlation coefficient depending on the type of material,  $a$  stands for the internal length scale,  $\nabla^2$  refers to the Laplacian operator,  $\tau_{kl}$  symbolizes the nonlocal stress tensor and  $\sigma_{kl}$  represents the classic stress tensor. The classical elasticity equation is accessible if parameter  $a$  takes zero value ( $e_0 a = 0$ ).

The constitutive equation is expressed as

$$\sigma_{ij} = 2\mu e_{ij} + [\lambda e_{kk} - \gamma(T - T_0)]\delta_{ij}, \quad (2)$$

in which  $\mu$  and  $\lambda$  represent the Lamé coefficients and  $\delta_{ij}$  refers to Kronecker's delta operator. Moreover,  $\theta = T - T_0$  stands for a temperature change with respect to reference temperature

$T_0$ ,  $e = \text{div } \vec{u}$  is the volumetric strain and  $\vec{u}$  denotes the displacement vector. Lamé's constants and shear modulus are defined by:

$$\lambda = \frac{E\nu}{(1+\nu)(1-2\nu)}, \quad \mu = \frac{E}{2(1+\nu)}. \quad (3)$$

The modified heat conduction equation that includes two phase lags is described as follows [2-4]:

$$\left(1 + \tau_\theta \frac{\partial}{\partial t}\right) (K\theta_{,i})_{,i} = \left(1 + \tau_q \frac{\partial}{\partial t} + \frac{1}{2}\tau_q^2 \frac{\partial^2}{\partial t^2}\right) \left(\rho C_E \frac{\partial \theta}{\partial t} + \gamma T_0 \frac{\partial e}{\partial t} - \rho Q\right), \quad (4)$$

where  $Q$  represents the heat source,  $\gamma = E\alpha_T/(1-2\nu)$ , in which  $\alpha_T$  is the thermal expansion constant,  $E$  denotes the module of elasticity,  $K$  implies the thermal conductivity,  $C_E$  refers to the specific heat and  $\rho$  symbolizes the density of material.

The theory of classical thermoelasticity, i.e. the Lord and Shulman model [1], and dual-phase-delay model [2-4] can be derived from Eq. (3) for the selection of different phase lag parameters  $\tau_\theta$  and  $\tau_q$ .

- By putting  $\tau_\theta = \tau_q = 0$  in Eq. (3), we get the nonlocal theory of coupled thermoelasticity (CTE).
- The generalized theory of nonlocal thermoelasticity (LS theory) can be obtained by putting  $\tau_\theta = 0$  and  $\tau_q = \tau_0$  ( $\tau_0$  refers to the relaxation time).
- The nonlocal dual-phase-lag model (DPL) is accessible when  $\tau_\theta$  falls within the interval  $[0, \tau_q]$ .

It is worth mentioning that if one of the thermo-physical characteristics ( $K, C_E$  and  $\rho$ ) depends on temperature, Eq. (3) is converted to a nonlinear partial differential equation.

### 3. PROBLEM FORMULATION

Fig. 1 displays the configuration of a thermoelastic rotating nanoscale beam. The considered nanobeam has thickness  $h$ , width  $b$  and length  $L$ . The  $x$ -axis lies in the axial direction of nanobeam and its width and thickness are in  $y$  and  $z$  directions, respectively. Initially, it is supposed that the nanobeam is stress free and the temperature is tentatively at  $T_0$ . The displacement components can be described as follows:

$$u = -z \frac{\partial w}{\partial x}, \quad v = 0, \quad w = w(x, t), \quad (5)$$

where  $w$  denotes the transverse deflection.

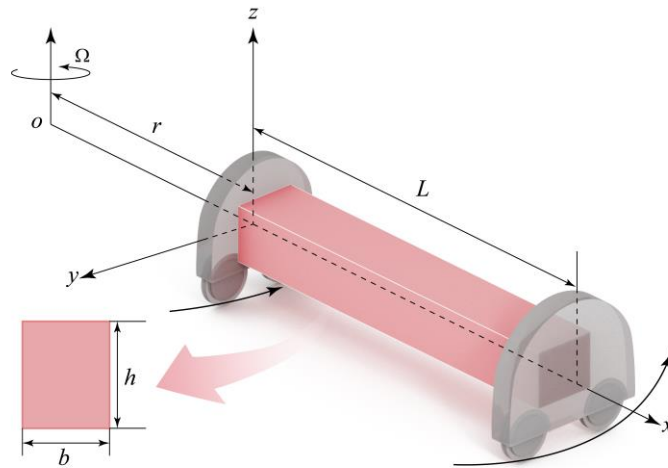


**Fig. 1** Schematic configuration of rotating nanobeam

Eq. (5) can be used to simplify the one dimension constitutive relationship (1) as

$$\sigma_x - \xi \frac{\partial^2 \sigma_x}{\partial x^2} = -E \left( z \frac{\partial^2 w}{\partial x^2} + \alpha_T \theta \right), \quad (6)$$

in which  $\sigma_x$  indicates the nonlocal axial thermal stress,  $\alpha_T = \alpha_t / (1 - 2\nu)$  and  $\xi = (e_0 a)^2$ . Bending moment  $M$  may be calculated by the following integration formula:

$$M(x, t) = \int_{-h/2}^{h/2} z \sigma_x dz. \quad (7)$$

Thereby, the following partial differential equation is satisfied by the bending moment after substituting Eq. (6) into Eq. (7)

$$M(x, t) - \xi \frac{\partial^2 M}{\partial x^2} = -EI \left( \frac{\partial^2 w}{\partial x^2} + \alpha_T M_T \right), \quad (8)$$

where  $EI$  and  $I = bh^3/12$  represent the bending rigidity of nanobeam and cross-sectional moment of inertia, respectively. In Eq. (8),  $M_T$  indicates the thermal moment of nanobeam and can be written by:

$$M_T = \frac{12}{h^3} \int_{-h/2}^{h/2} \theta(x, z, t) z dz. \quad (9)$$

It is assumed that the nanoscale beam is distributed by a transversely varying force  $q(x, t)$  and, therefore, the transversal equation of motion can be written as [37]

$$\frac{\partial^2 M}{\partial x^2} = -q(x, t) + \rho b h \frac{\partial^2 w}{\partial t^2}, \quad (10)$$

It is supposed that the nanobeam rotates with angular velocity  $\Omega$  (about the axis which is parallel to  $z$  axis) centered at a small distance  $r$  from the left edge of the nanobeam. Centrifugal tension force  $R(x)$  is introduced as a result of rotation. In this case, the equation of motion (10) is given as [41]

$$\frac{\partial^2 M}{\partial x^2} + \frac{\partial}{\partial x} \left( R(x) \frac{\partial w}{\partial x} \right) + q(x, t) = \rho b h \frac{\partial^2 w}{\partial t^2} \quad (11)$$

Centrifugal force  $R$  vanishes when angular velocity  $\Omega$  is equal to zero and the nanobeam is in stationary state.

The centrifugal stiffening effect can be modeled by including axial-type load  $R(x)$  which can be described as [41, 42]

$$R(x) = \int_x^L \rho A \Omega^2 (r + x) dx \quad (12)$$

in which  $x$  represents the distance from the origin (see Fig. 1). Parameter  $r$  refers to the distance from the rotation axis to the left edge of the nanobeam (a hub radius in Fig. 1). After some computations, Eq. (12) can be simplified as

$$\begin{aligned} R(x) &= \frac{\rho A \Omega^2}{2} [(L + r)^2 - (L + x)^2] \\ &= \frac{\rho A \Omega^2}{2} [(r - x)(2L + r + x)] \end{aligned} \quad (13)$$

For calculating bending moment  $M(x, t)$ , Eqs. (11) and (13) can be utilized

$$M(x, t) = \xi \left( \rho A \frac{\partial^2 w}{\partial t^2} - q(x, t) - \frac{\partial}{\partial x} \left( R(x) \frac{\partial w}{\partial x} \right) \right) - EI \left( \frac{\partial^2 w}{\partial x^2} + \alpha_T M_T \right) \quad (14)$$

If moment  $M$  is omitted in Eqs. (11) and (14), the governing equation can be expressed as

$$\left[ \frac{\partial^4}{\partial x^4} + \frac{\rho A}{EI} \frac{\partial^2}{\partial t^2} \left( 1 - \xi \frac{\partial^2}{\partial x^2} \right) \right] w - \frac{1}{EI} \left( 1 - \xi \frac{\partial^2}{\partial x^2} \right) \left[ q + \frac{\partial}{\partial x} \left( R(x) \frac{\partial w}{\partial x} \right) \right] + \alpha_T \frac{\partial^2 M_T}{\partial x^2} = 0 \quad (15)$$

In the absence of heat source ( $Q = 0$ ), the modified heat conduction relation (4) can be defined as

$$\left( 1 + \tau_\theta \frac{\partial}{\partial t} \right) \nabla \cdot (K_x \nabla \theta) = \left( 1 + \tau_q \frac{\partial}{\partial t} + \frac{\tau_q^2}{2} \frac{\partial^2}{\partial t^2} \right) \frac{\partial}{\partial t} \left( \rho C_E \theta - \gamma T_0 z \frac{\partial^2 w}{\partial x^2} \right) \quad (16)$$

#### 4. THERMAL PROPERTIES OF MATERIALS

The identification of nonlinear problems will be carried out if the material properties are temperature-dependent which means specific heat  $C_E$  and thermal conductivity  $K$  depend upon the temperature distribution [28]. In the current work, it is assumed that other physical parameters are constant and not dependent on the temperature changes [43]. The material's thermal conductivity  $K$  is supposed to be defined by a linear function of temperature change [44] as follows:

$$K_x = K_x(\theta) = K_0(1 + K_1 \theta), \quad (17)$$

in which parameter  $K_0$  denotes the thermal conductivity at reference temperature  $T_0$  and  $K_1$  denotes a factor that characterizes thermal conductivity variability.

By substituting Eq. (17) into Eq. (16), the partial nonlinear differential equation is obtained in the form

$$K_0 \left(1 + \tau_\theta \frac{\partial}{\partial t}\right) \nabla \cdot \left((1 + K_1 \theta) \nabla \theta\right) = \left(1 + \tau_q \frac{\partial}{\partial t} + \frac{\tau_q^2}{2} \frac{\partial^2}{\partial t^2}\right) \frac{\partial}{\partial t} \left(\rho C_E \theta - \gamma T_0 z \frac{\partial^2 w}{\partial x^2}\right) \quad (18)$$

The previous equation can be converted to a linear equation by defining the mapping [43]

$$K_0 \psi = \int_0^\theta K_x(\theta) d\theta, \quad (19)$$

After inserting Eq. (17) into Eq. (19) and computing the integration, we have [43]

$$\psi = \theta \left(1 + \frac{1}{2} K_1 \theta\right). \quad (20)$$

Through differentiating relation Eq. (20) with regard to distance variable and also with respect to time variable  $t$ , the following relationships are deduced

$$\nabla \psi = \frac{K_r(\theta)}{K_0} \nabla \theta, \quad (21)$$

$$\frac{\partial \psi}{\partial t} = \frac{K_r(\theta)}{K_0} \frac{\partial \theta}{\partial t}. \quad (22)$$

By employing Eqs. (21) and (22), therefore, the heat conduction equation (18) is simplified to

$$\left(1 + \tau_\theta \frac{\partial}{\partial t}\right) \left(\frac{\partial^2}{\partial x^2} + \frac{\partial^2}{\partial z^2}\right) \psi = \left(1 + \tau_q \frac{\partial}{\partial t} + \frac{1}{2} \tau_q^2 \frac{\partial^2}{\partial t^2}\right) \frac{\partial}{\partial t} \left(\eta \psi - \frac{\gamma T_0}{K} z \frac{\partial^2 w}{\partial x^2}\right). \quad (23)$$

in which  $1/\eta = K/\rho C_E$  stands for thermal diffusivity.

## 5. SINUSOIDAL SOLUTION

In order to calculate the solution of the problem, we take the temperature change response as a sinusoidal solution

$$\{\psi, \theta\}(x, z, t) = \{\Psi, \Theta\}(x, t) \sin\left(\frac{\pi}{h} z\right). \quad (24)$$

substituting Eq. (24) into Eqs. (14), (15) and (23), which leads to

$$\left[\frac{\partial^4}{\partial x^4} + \frac{\rho A}{EI} \frac{\partial^2}{\partial t^2} \left(1 - \xi \frac{\partial^2}{\partial x^2}\right)\right] w - \frac{1}{EI} \left(1 - \xi \frac{\partial^2}{\partial x^2}\right) q + \frac{24\alpha_T}{\pi^2 h} \frac{\partial^2 \Psi}{\partial x^2} = 0, \quad (25)$$

$$M(x, t) = \xi \left(\rho A \frac{\partial^2 w}{\partial t^2} - q\right) - EI \left(\frac{\partial^2 w}{\partial x^2} + \frac{24T_0 \alpha_T}{\pi^2 h} \Theta\right), \quad (26)$$

$$\left(1 + \tau_\theta \frac{\partial}{\partial t}\right) \left(\frac{\partial^2}{\partial x^2} - \frac{\pi^2}{h^2}\right) \Psi = \left(1 + \tau_q \frac{\partial}{\partial t} + \frac{1}{2} \tau_q^2 \frac{\partial^2}{\partial t^2}\right) \frac{\partial}{\partial t} \left(\eta \Psi - \frac{\gamma T_0 \pi^2 h}{24K} \frac{\partial^2 w}{\partial x^2}\right). \quad (27)$$

Some nondimensional variables are provided below for the sake of generality

$$\begin{aligned} \{u', x', L', w', z', h', b'\} &= \eta c \{u, x, L, w, z, h, b\}, & \{t', \tau'_q, \tau'_\theta\} &= \eta c^2 \{t, \tau_q, \tau_\theta\}, \\ \xi' &= \eta^2 c^2 \xi, & \{\Theta', \Psi'\} &= \frac{1}{T_0} \{\Theta, \Psi\}, & M' &= \frac{1}{\eta c EI} M, & q' &= \frac{A}{EI} q, & c^2 &= \frac{E}{\rho}. \end{aligned} \quad (28)$$

After introducing dimensionless parameters in Eqs. (25) to (27), one can obtain

$$\left[\frac{\partial^4}{\partial x^4} + \frac{12}{h^2} \frac{\partial^2}{\partial t^2} \left(1 - \xi \frac{\partial^2}{\partial x^2}\right)\right] w - \left(1 - \xi \frac{\partial^2}{\partial x^2}\right) \left[q + \frac{\partial}{\partial x} \left(R(x) \frac{\partial w}{\partial x}\right)\right] + \frac{24T_0 \alpha_T}{\pi^2 h} \frac{\partial^2 \Theta}{\partial x^2} = 0 \quad (29)$$



$$\left(1 + \tau_\theta \frac{\partial}{\partial t}\right) \left(\frac{\partial^2}{\partial x^2} - \frac{\pi^2}{h^2}\right) \Psi = \left(1 + \tau_q \frac{\partial}{\partial t} + \frac{\tau_q^2}{2} \frac{\partial^2}{\partial t^2}\right) \frac{\partial}{\partial t} \left(\Psi - \frac{\gamma \pi^2 h}{24K\eta} \frac{\partial^2 w}{\partial x^2}\right) \quad (30)$$

$$M(x, t) = \frac{12\xi}{h^2} \frac{\partial^2 w}{\partial t^2} - \xi \left[ q + \frac{\partial}{\partial x} \left( R(x) \frac{\partial w}{\partial x} \right) \right] - \frac{\partial^2 w}{\partial x^2} - \frac{24T_0 \alpha_T}{\pi^2 h} \Theta \quad (31)$$

In Eqs. (29)-(31), the primes are omitted for the sake of simplicity.

A specific type of external transverse load is now taken into account. It is considered that the vertical load decays exponentially with time, acting towards the thickness of the beam [45] as follows

$$q(x, t) = -q_0 (1 - \delta e^{-\beta t}) \quad (32)$$

where  $q_0$  is the magnitude of the dimensionless point load and  $\beta$  is the dimensionless decaying parameter of the external force, respectively ( $\delta = 0$  can be used in the case of uniform distributed force).

It is also assumed that the system works at constant rotating speed and centrifugal tension load  $R(x)$  is considered to have its maximum value (at  $x = 0$ ) which takes the following form [41]

$$R_{max} = \int_0^L \rho A \Omega^2 (r + x) dx = \frac{1}{2} \rho A \Omega^2 L (2r + L) \quad (33)$$

Thereby, the equation of motion (29) can be described as

$$\left[ \frac{\partial^4}{\partial x^4} + \frac{12}{h^2} \frac{\partial^2}{\partial t^2} \left( 1 - \xi \frac{\partial^2}{\partial x^2} \right) \right] w - \left( 1 - \xi \frac{\partial^2}{\partial x^2} \right) \left[ q + \frac{6L\Omega^2(2r+L)}{h^2} \frac{\partial^2 w}{\partial x^2} \right] + \frac{24T_0 \alpha_T}{\pi^2 h} \frac{\partial^2 \Theta}{\partial x^2} = 0 \quad (34)$$

The bending moment in Eq. (31) may also be defined as

$$M(x, t) = \frac{12\xi}{h^2} \frac{\partial^2 w}{\partial t^2} - \xi \left[ q + \frac{6L\Omega^2(2r+L)}{h^2} \frac{\partial^2 w}{\partial x^2} \right] - \frac{\partial^2 w}{\partial x^2} - \frac{24T_0 \alpha_T}{\pi^2 h} \Theta \quad (35)$$

The initial conditions are supposed to be

$$\Psi(x, 0) = \frac{\partial \Psi(x, 0)}{\partial t} = 0, \quad w(x, 0) = \frac{\partial w(x, 0)}{\partial t} = 0. \quad (36)$$

The nanobeam subjects to the following boundary conditions:

- Doubly-clamped ends with the following conditions

$$w(x, t)|_{x=0,L} = 0, \quad \frac{\partial w(x, t)}{\partial x} \Big|_{x=0,L} = 0. \quad (37)$$

- The nanobeam is harmonically heated as

$$\Theta(0, t) = \Theta_0 \cos(\omega t), \quad \omega > 0, \quad (38)$$

in which  $\Theta_0$  is its amplitude and  $\omega$  denotes the thermal angular frequency. In the case of  $\omega = 0$ , the above condition is utilized for thermal shock loading.

Using Eq. (15) and Eq. (20) yields

$$\Psi(0, t) = \Theta_0 \cos(\omega t) + \frac{1}{2} K_1 [\Theta_0 \cos(\omega t)]^2. \quad (39)$$

- The surface  $x = L$  is assumed to be thermally isolated

$$\frac{\partial \Psi(L, t)}{\partial x} = 0. \quad (40)$$

## 6. LAPLACE TRANSFORM STRATEGY

Using Laplace technique, Eqs. (30), (34) and (35) are converted to the following equations

$$\left[ \left( 1 + \frac{6\xi L \Omega^2 (2r+L)}{h^2} \right) \frac{d^4}{dx^4} - \left( \frac{12\xi s^2}{h^2} + \frac{6L \Omega^2 (2r+L)}{h^2} \right) \frac{d^2}{dx^2} + \frac{12s^2}{h^2} \right] \bar{w} = -\frac{24T_0 \alpha_T}{\pi^2 h} \frac{d^2 \bar{\theta}}{dx^2} - \bar{g}(s) \quad (41)$$

$$(1 + \tau_\theta s) \left( \frac{d^2}{dx^2} - \frac{\pi^2}{h^2} \right) \bar{\Psi} = s(1 + \tau_q s + s^2 \tau_q^2 / 2) \left( \bar{\Psi} - \frac{\gamma \pi^2 h}{24K\eta} \frac{d^2 \bar{w}}{dx^2} \right) \quad (42)$$

$$\bar{M}(x, s) = \frac{12\xi s^2}{h^2} \bar{w} - \left( 1 + \frac{6\xi L \Omega^2 (2r+L)}{h^2} \right) \frac{d^2 \bar{w}}{dx^2} - \frac{24T_0 \alpha_T}{\pi^2 h} \bar{\theta} - \xi \bar{g}(s) \quad (43)$$

where  $\bar{g}(s) = q_0 \left( \frac{1}{s} - \frac{\delta}{\beta+s} \right)$ .

The following differential equation can be obtained once function  $\bar{\theta}$  is extracted from Eqs. (41) and (42)

$$\left[ \frac{d^6}{dx^6} - A \frac{d^4}{dx^4} + B \frac{d^2}{dx^2} - C \right] \bar{w} = A_5 \bar{g}(s) / A_1 \quad (44)$$

where

$$\begin{aligned} A &= \frac{1}{A_1} (A_5 A_1 + A_2 + A_4 A_6), \quad B = \frac{1}{A_1} (A_5 A_2 + A_3), \quad C = \frac{A_5 A_3}{A_1}, \\ A_1 &= \left( 1 + \frac{6\xi L \Omega^2 (2r+L)}{h^2} \right), \quad A_2 = \left( \frac{12\xi s^2}{h^2} + \frac{6L \Omega^2 (2r+L)}{h^2} \right), \quad A_4 = \frac{24T_0 \alpha_T}{\pi^2 h}, \\ A_3 &= \frac{12s^2}{h^2}, \quad A_5 = \frac{\pi^2}{h^2} + \frac{s(1+\tau_q s + s^2 \tau_q^2 / 2)}{1+\tau_\theta s}, \quad A_6 = \frac{s(1+\tau_q s + s^2 \tau_q^2 / 2)}{1+\tau_\theta s} \left( \frac{\gamma \pi^2 h}{24K\eta} \right). \end{aligned} \quad (45)$$

Then the general solution for  $\bar{w}$  can be achieved by solving the differential Eq. (44) as follows

$$\bar{w}(x, s) = \sum_{j=1}^3 (C_j e^{-m_j x} + C_{j+3} e^{m_j x}) - \frac{A_5 \bar{g}(s)}{C A_1} \quad (46)$$

From the given boundary conditions, undetermined parameters  $C_j$ , ( $j = 1, 2, \dots, 6$ ), can be calculated. Parameters  $m_1^2$ ,  $m_2^2$  and  $m_3^2$  also satisfy the following equation

$$m^6 - A m^4 + B m^2 - C = 0 \quad (47)$$

Eq. (46) is incorporated into Eq. (41) and yields

$$\bar{\Psi}(x, s) = -\frac{1}{A_4 A_5} \left[ A_1 \frac{d^4 \bar{w}}{dx^4} - (A_2 + A_4 A_6) \frac{d^2 \bar{w}}{dx^2} + A_3 \bar{w} + \bar{g}(s) \right] \quad (48)$$

With the help of Eq. (46), the solution of Eq. (48) can be simplified as

$$\bar{\Psi}(x, s) = \sum_{j=1}^3 H_j (C_j e^{-m_j x} + C_{j+3} e^{m_j x}) - H_4, \quad (49)$$

where

$$H_j = -\frac{1}{A_4 A_5} [A_1 m_j^4 - (A_2 + A_4 A_6) m_j^2 + A_3], \quad H_4 = \frac{\bar{g}(s)(A_4 - C)}{C A_4 A_5} \quad (50)$$

Bending moment  $\bar{M}$  is determined from (43) using the solutions (46) and (49)

$$\bar{M}(x, s) = \sum_{j=1}^3 L_j (C_j e^{-m_j x} + C_{j+3} e^{m_j x}) + L_4 \quad (51)$$

where

$$L_j = -(A_1 m_j^2 + A_4 H_j - A_0), \quad L_4 = \bar{g}(s) \left( A_4 H_4 - \frac{A_0 A_5}{C A_1} - \xi \right), \quad A_0 = \frac{12 \xi s^2}{h^2} \quad (52)$$

Axial displacement  $\bar{u}$  can be calculated by using Eq. (46)

$$\bar{u} = -z \frac{d\bar{w}}{dx} = z \sum_{j=1}^3 m_j (C_j e^{-m_j x} - C_{j+3} e^{m_j x}). \quad (53)$$

Boundary conditions (37)-(40) are reduced in the Laplace transform field to

$$\bar{w}(x, s)|_{x=0,L} = 0, \quad \left. \frac{d^2 \bar{w}(x, s)}{dx^2} \right|_{x=0,L} = 0, \quad (54)$$

$$\bar{\Psi}(x, s)|_{x=0} = \Theta_0 \left[ \frac{s}{s^2 + \omega^2} + \frac{K_1 (s^2 + 2\omega^2)}{2s(s^2 + 4\omega^2)} \right] = \bar{G}(s), \quad (55)$$

$$\left. \frac{d\bar{\Theta}}{dx} \right|_{x=L} = 0. \quad (56)$$

By applying these conditions in Eqs. (46) and (49), the following system of equations are obtained

$$\sum_{j=1}^3 (C_j + C_{j+3}) = \frac{A_5 \bar{g}(s)}{C A_1} \quad (57)$$

$$\sum_{j=1}^3 (C_j e^{-m_j L} + C_{j+3} e^{m_j L}) = \frac{A_5 \bar{g}(s)}{C A_1} \quad (58)$$

$$\sum_{j=1}^3 m_j^2 (C_j + C_{j+3}) = \frac{A_5 \bar{g}(s)}{C A_1} \quad (59)$$

$$\sum_{j=1}^3 m_j^2 (C_j e^{-m_j L} + C_{j+3} e^{m_j L}) = \frac{A_5 \bar{g}(s)}{C A_1} \quad (60)$$

$$\sum_{j=1}^3 H_j (C_j + C_{j+3}) = H_4 + \bar{G}(s), \quad (61)$$

$$\sum_{j=1}^3 m_j H_j (C_j e^{-m_j L} - C_{j+3} e^{m_j L}) = 0, \quad (62)$$

Parameters  $C_j$ , ( $j = 1, 2, \dots, 6$ ) are unknown and have to be determined and, thereby, the analytical solutions for the physical parameters in the Laplace domain can be achieved. It is difficult to take the Laplace inversion of the complicated transformed field variables expressions. Within the next section, the results are evaluated numerically using the expansion technique of the Fourier series.

Temperature  $\bar{\theta}$  can be obtained by solving Eq. (20) after applying the Laplace transform as

$$\bar{\theta}(x, s) = \sin\left(\frac{\pi}{h} z\right) \left[ \frac{-1 + \sqrt{1 + 2K_1 \bar{\psi}}}{K_1} \right] \quad (63)$$

### 7. LAPLACE TRANSFORM INVERSION

With the aim of solutions in the physical domain, at last, we invert the transformation of Laplace to the functions that govern the motion of the system. We now follow a numerical overlay strategy based on an extension of the Fourier series [46]. Any functions in

the Laplace domain, i.e.  $\bar{g}(x, s)$ , is transferred to the time domain, i.e.  $g(x, t)$ , by using the following procedure:

$$g(x, t) = \frac{e^{ct}}{t} \left\{ \frac{1}{2} \bar{g}(x, c) + \operatorname{Re} \left[ \sum_{n=1}^N (-1)^n \bar{g} \left( x, c + \frac{in\pi}{t} \right) \right] \right\}, \quad (64)$$

where  $N$  represents a large value denoting the number of truncated terms in the original Fourier series and can be selected to satisfy

$$e^{ct} \operatorname{Re} \left\{ (-1)^n \bar{g} \left( x, c + \frac{in\pi}{t} \right) \right\} \leq \varepsilon_1, \quad (65)$$

in which  $\varepsilon_1$  is a small positive integer corresponds to achieve the desired accuracy. Various numerical studies demonstrated that parameter  $c$  can be determined as  $ct \approx 4.7$  for appropriate convergence [47].

## 8. RESULTS AND DISCUSSION

Throughout this section, some discussions and numerical results are provided to illustrate the general response of the problem. Moreover, the numerical examples are presented to explore the impacts of the physical fields analyzed with three appropriate parameters. Specific physical parameters are taken into consideration from the published works in the literature for computational purposes. In our analysis, the following properties are utilized for silicon-based material:

$$E = 169 \text{ GPa}, \quad \rho = 2330 \left( \frac{\text{kg}}{\text{m}^3} \right), \quad C_E = 713 \left( \frac{\text{J}}{\text{kg K}} \right), \\ \alpha_T = 2.59 \times 10^{-9} \left( \frac{1}{\text{K}} \right), \quad \nu = 0.22, \quad T_0 = 293 \text{ K}, \quad K = 156 \left( \frac{\text{W}}{\text{mK}} \right).$$

We consider a nanobeam with dimensionless parameters as given in Eq. (24). The following values are set in our calculations, i.e.,  $L/h = 10$  and  $b/h = 0.5$ . The dimensionless length is taken as  $L = 1$  and it is assumed that  $t = 0.1$ .

As mentioned before, a linear function of temperature change  $\theta$  is considered for the thermal conductivity of the material (see Eq. (13)). Figs. 2-5 show the variations of nondimensional displacement, bending moment and temperature gradient for different values of  $K_1$ -parameter to illustrate the thermal properties of the nanobeam that vary in terms of temperature variable  $\theta$ . Two different thermal conduction parameters will be considered. When the thermal conductivity depends on temperature, values  $K_1 = -1$  and  $K_1 = -0.5$  are taken into account. If the thermal conductivity remains constant, then  $K_1$  is equal to zero. It is assumed that the other parameters are fixed and take the values  $\xi = 0.01$ ,  $\omega = 5$ ,  $\Omega = 0.3$ ,  $\tau_q = 0.02$  and  $\tau_\theta = 0.01$ .

From the illustrative results, it is observed that any change in parameter  $K_1$  has a remarkable influence on all studied fields that proves that the consideration of variable thermal conductivity is essential for this kind of analysis. It is also noted that the behavior of nanostructures are dependent on temperature changes and with the increase in the external temperatures, the results of small-scale nonlocal theories also increase.

The variation of deflection  $w$  versus distance  $x$  for different values of thermal conductivity parameter  $K_1$  is shown in Fig. 2. As can be seen, increasing the values of parameter  $K_1$  results

in decreasing lateral vibration  $w$ . Fig. 2 illustrates that the deflection distribution  $w$  has zero values at both ends (i.e. disappears) and meets the limit conditions of the rotating nanobeam at  $x = 0$  and  $x = L$ . Temperature  $\theta$  is also depicted in terms of parameter  $K_1$  in Fig. 3. Temperature  $\theta$  will decrease while distance  $x$  becomes larger to drive towards wave propagation, as shown in Fig. 3.

From theoretical experiments, it is found that the thermal conductivity of pure metals decreases as the temperature increases. However, the thermal conductivity drops dramatically as the temperatures exceed absolute zero [48]. Fig. 3 indicates that any reduction in parameter  $K_1$  results in increasing temperature values  $\theta$ . This phenomenon is verified by the experimental results reported by Abo-Dahab et al. [49].

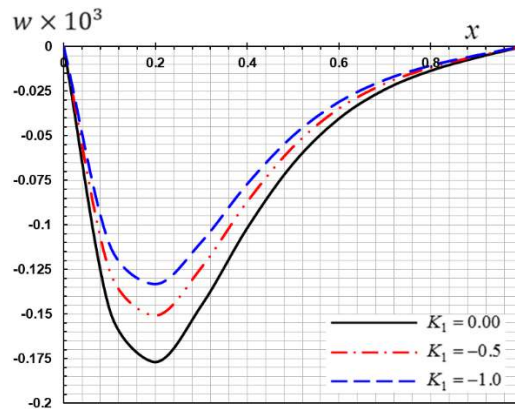


**Fig. 2** Deflection  $w$  under the influence of variable thermal properties

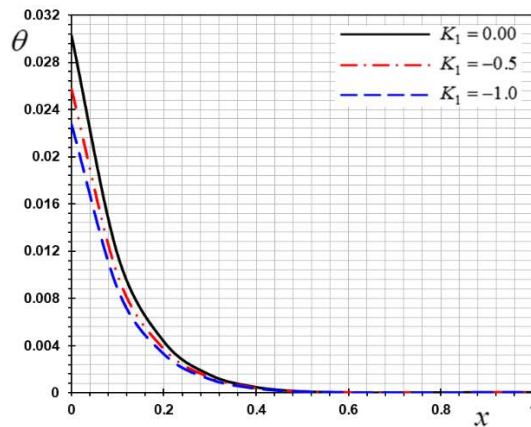


**Fig. 3** Temperature  $\theta$  under the influence of variable thermal properties

Fig. 4 demonstrates that the values of displacement decrease from 0 to 0.3 and consequently in the range 0.3 to 0.8 shift upward to the highest amplifications. In addition, the

values of  $u$  vary linearly in the last interval  $0.8 \leq x \leq 1$  of wave propagation. It should be noted that the displacement distribution is highly influenced by the variation of parameter  $K_1$ .

According to Fig. 5, the effect of parameter  $K_1$  is revealed as increasing the distribution of bending moment  $M$  which implies that the impact of thermal conductivity variation cannot be disregarded [48]. The mechanical characteristics of the nanobeam emphasize that the wave propagates in the medium with finite speed [49].

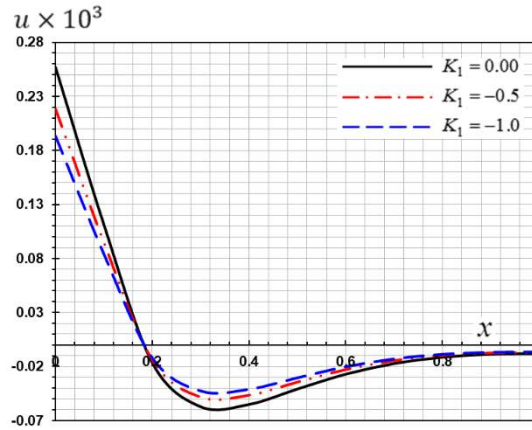


**Fig. 4** Displacement  $u$  under the influence of variable thermal properties

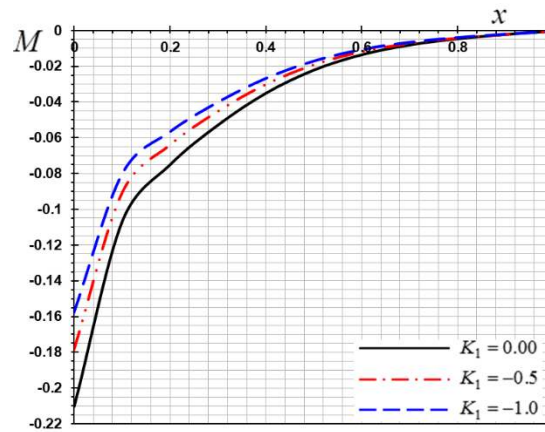


**Fig. 5** Bending moment  $M$  under the influence of variable thermal properties

In the second case, the influence of angular rotation velocity  $\Omega$  on the dimensionless field quantities is illustrated. It is supposed that our findings are consistent with both nonlocal parameter  $\xi$ , the angular excitation of thermal load  $\omega$ , and phase lags  $\tau_q$  and  $\tau_\theta$ . Our calculations are performed using fixed values for system parameters as  $\xi = 0.1$ ,  $\omega = 5$ ,  $\tau_q = 0.02$  and  $\tau_\theta = 0.01$ .

The variations of the fields studied for three assigned values of rotational speed ( $\Omega = 0, 0.1, 0.3$ ) are shown in Figs. 6-9. In the case of stationary nanobeam, the rotational speed is set to be zero ( $\Omega = 0$ ), as a special case in our simulations.

The variation of angular speed  $\Omega$  which cases the variation in deflection  $w$ , is depicted in Fig. 6. As indicated, this parameter is found to have a substantial effect on the distribution of deflection  $w$  by comparing the results of stationary beam with rotating one. When angular velocity  $\Omega$  becomes larger, deflection  $w$  takes smaller values. The obtained results are consistent with those reported by Ebrahimi et al. [50].

The variation in temperature  $\theta$  with respect to distance  $x$  is verified by assuming different values for rotational speed  $\Omega$ , as demonstrated in Fig. 7.

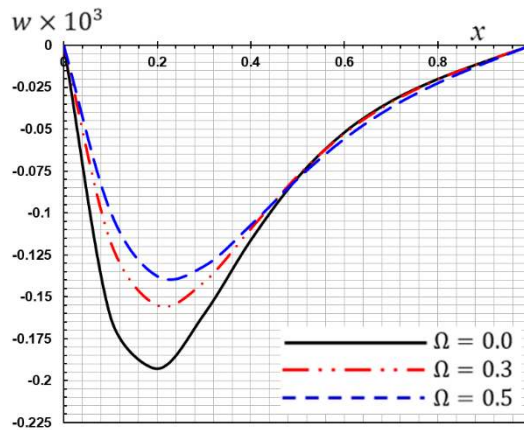


**Fig. 6** Deflection  $w$  vs angular velocity  $\Omega$

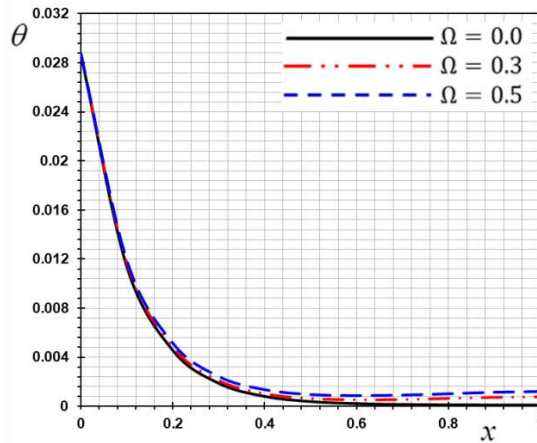


**Fig. 7** Temperature  $\theta$  vs angular velocity  $\Omega$

Clearly, the temperature shifts upward as angular velocity  $\Omega$  increases which is also consistent with the observations of Ebrahimi and Shafie [50, 51].

Fig. 8 presents a survey of the impact of angular speed  $\Omega$  on the variation of displacement  $u$ . It is inferred that the curves that reflect the displacement field are influenced by the rotation. This figure shows that at certain ranges, by increasing the rotation speed, the distribution of displacement  $u$  sharply decreases at first and then slightly increases. Fig. 9 shows the influence of the variation of angular velocity  $\Omega$  on the distribution of bending moment  $M$  for rotating nanobeams. It is observed from the figure that the rotation of the nanobeam has a great effect on the values of bending moment and the amplitude of the moment becomes larger by increasing angular velocity  $\Omega$ .

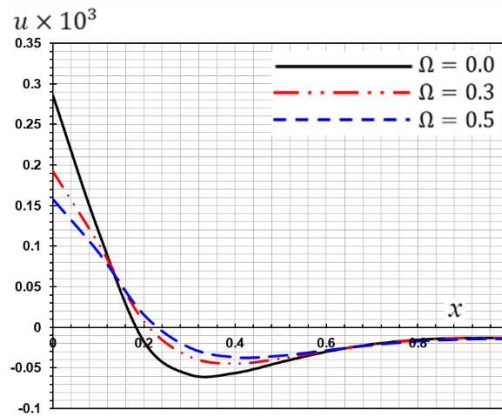


**Fig. 8** Displacement  $u$  vs angular velocity  $\Omega$

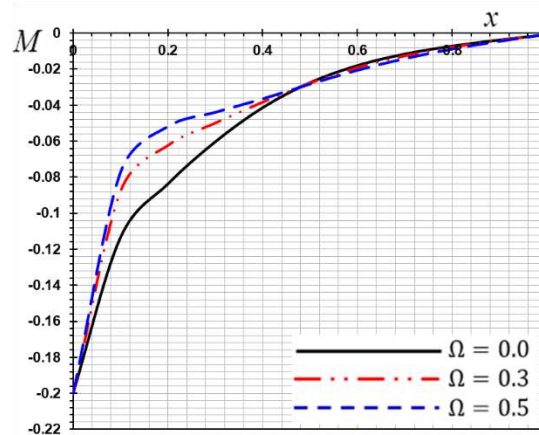


**Fig. 9** Bending moment  $M$  vs angular velocity  $\Omega$

One of the objectives of this study is to explore the mechanical features of certain nano-devices such as nano-turbine blades [52] in the presence of temperature field and angular velocity which may provide valuable insights for designers and engineers. From the previous observations, one can also deduce the major impact of rotation on the



distribution of physical properties of such devices. It should be emphasized that the findings are in line with the earlier results in Refs. [53-55].

When the values of parameters  $(\omega, K_1, \Omega, \tau_q, \tau_\theta)$  are fixed, the effect of the nonlocal parameter  $\xi$  on the non-dimensional field variables can be examined. Through Figs. 10-13, along the axial direction, the thermoelastic behavior of rotating nanobeam is shown by plotting the variations of displacement  $u$ , bending moment  $M$ , deflection  $w$  and temperature  $\theta$ . The values of nonlocal parameter are considered to be  $\xi = 0$  (classical theory),  $\xi = 0.01$  and  $\xi = 0.03$  for comparison. The figures exhibit that the nonlocality of the nanobeam has distinct influences on all fields studied and illustrates the difference between classical thermoelasticity theories and nonlocal ones.

For various three assigned values of nonlocal scaling parameter  $\xi$ , Fig. 10 shows different curves for the deflection of non-rotating nanobeam. It can be seen that with an increase in the nonlocal parameter, the deflection becomes very small and the dispersed nature turns into a non-dispersed form. The temperature distributions are also shown for various nonlocal scaling parameter versus axial direction  $x$ , in Fig. 11. It is concluded that the temperature convergence can be achieved by increasing the nonlocal scaling parameter. Fig. 12 demonstrates that the displacement amplitude increases with the nonlocal parameter due to the inclusion of nonlocality in the thermoelastic model. The influence of the nonlocal parameter  $\xi$  on the variation of bending moment is presented in Fig. 13. One observes that as the nonlocal scale parameter increases, the bending moment tends to decrease substantially.

It is worth mentioning that our findings and conclusions are in agreement with those reported in the literature [56]. The results typically confirm that one should expect significant diversity in the results by considering the nonlocality of nanobeam rather than classical one. The distinction between classical thermoelasticity models and nonlocal thermoelasticity theories in thermal fields is justified [57]. In the nanoscale systems and devices, the impact of this parameter should also be taken into account.

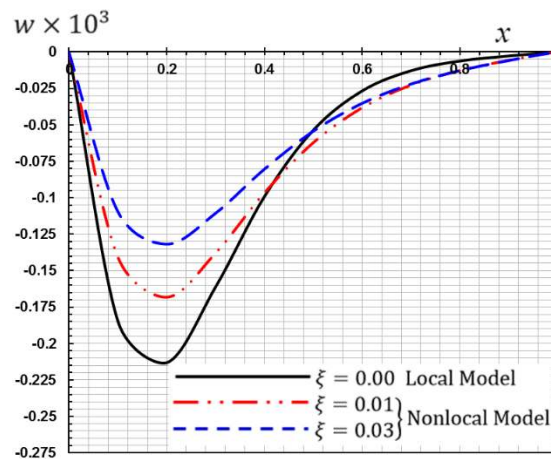


**Fig. 10** Deflection  $w$  distribution vs nonlocal parameter  $\xi$

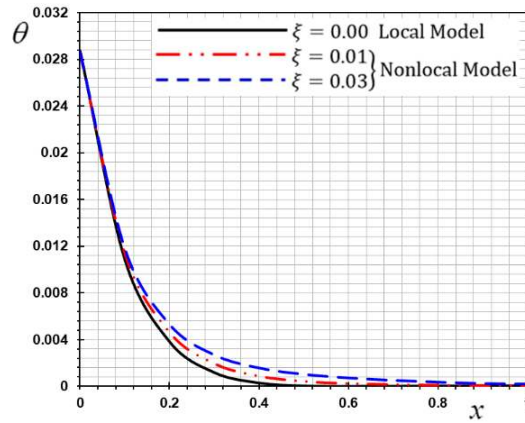


Fig. 11 Temperature  $\theta$  distribution vs nonlocal parameter  $\xi$

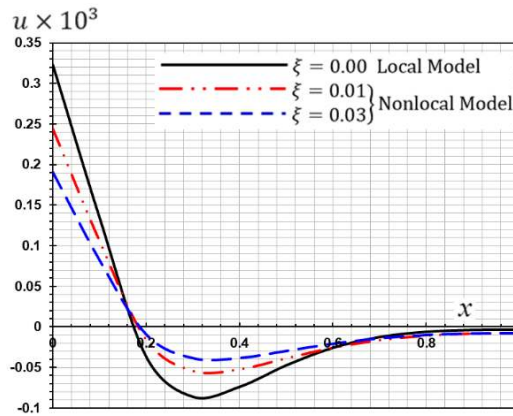


Fig. 12 Displacement  $u$  distribution vs nonlocal parameter  $\xi$

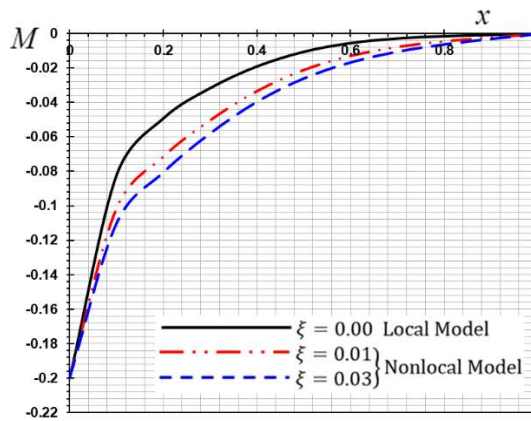


Fig. 13 Bending moment  $M$  distribution vs nonlocal parameter  $\xi$

As the last effort in this research, the variations of different fields variables in terms of the point load  $q_0$  are plotted in Figs. 14-17. There are three different non-dimensional values for point load  $q_0$  which are taken into account for the sake of comparison. The plotted curves show the distinct effect of the point load on the results. In the case of uniform distributed load, it is assumed that  $\delta = 0$ , and for the point load with exponential decay in time, it is considered that  $\delta = 1$ . Clearly, the difference between the outcomes becomes more significant with increasing amplitude of point load  $q_0$ . Figs. 14-17 indicate that there is a greater discrepancy between  $u$  and  $w$  quantities by increasing the point load compared to those for bending moment and temperature gradient.

It is also noted from these figures that the absolute values of the field variables become larger when the exponential decay with respect to time is considered for point load  $q_0$  [58, 59].

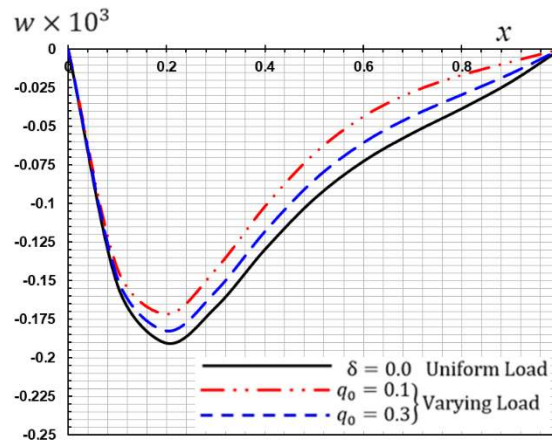


Fig. 14 Deflection  $w$  under the influence of point load  $q_0$

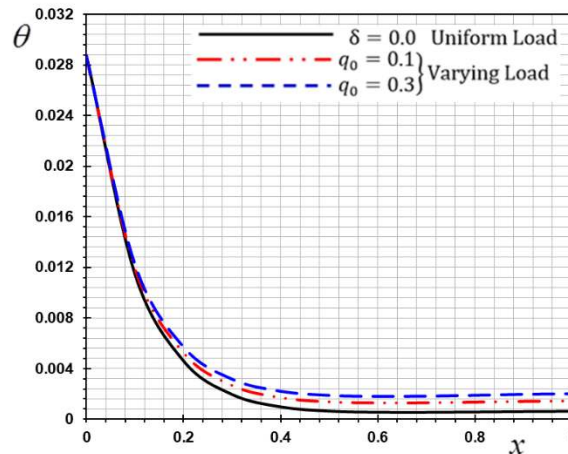
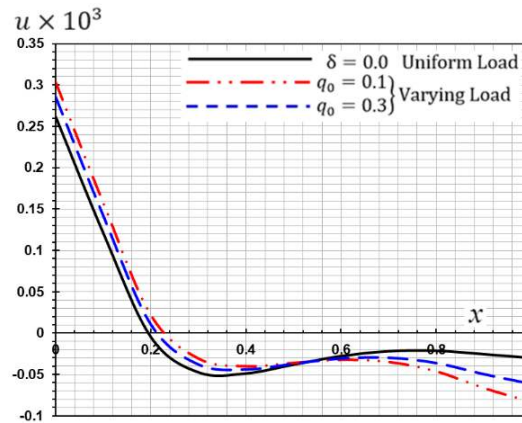
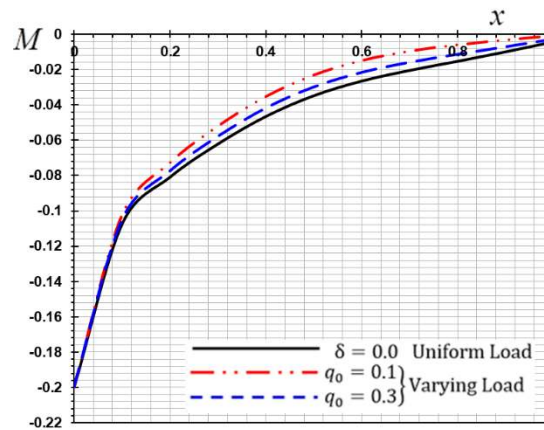


Fig. 15 Temperature  $\theta$  under the influence of point load  $q_0$



**Fig. 16** Displacement  $u$  under the influence of point load  $q_0$



**Fig. 17** Bending moment  $M$  under the influence of point load  $q_0$

## 9. CONCLUSIONS

This research focused on the wave dispersion behavior of rotating nanobeam on the basis of the nonlocal elasticity theory in conjunction with generalized thermoelasticity with phase-lag. The systems of governing equations were derived in the context of the Euler-Bernoulli beam theory. The thermal conductivity of nanobeam and modulus of elasticity were considered to be temperature-dependent. For a uniform rotating nanobeam, the governing equations were extracted considering the variability of thermal conductivity and nonlocal scale effect. The nanobeam surface was assumed to be thermally loaded with uniformly heat source by considering the exponential decay with time. The effects of dynamic load, nonlocal parameter, rotating speed and thermal conductivity variations on the field variables were graphically described and examined. Our findings showed the following important results:

- The variation of the thermal conductivity affects the wave propagation rate of all of field variables. Physical fields strongly depend on the variation of the thermal conductivity.
- The dependency of the thermal conductivity on the temperature causes a significant influence on the mechanical and thermal interactions.
- The nonlocal parameter effects are considered to be significant on all fields studied.
- The presence of dynamic load has a considerable impact on the results of all physical quantities.
- There are significant differences between the results of point load with exponential decay and those obtained in the case of uniformly distributed one. The thermoelastic stresses and temperature gradient, on the other hand, are highly dependent on the angular frequency of the thermal loading.

Current research may be used in applications including micro and nano mechanical gears, micro-mirrors for light guiding purposes in image projection devises, micro-turbine blades, micro accelerometers (Fig. 18), resonators, frequency filters and relay switches.

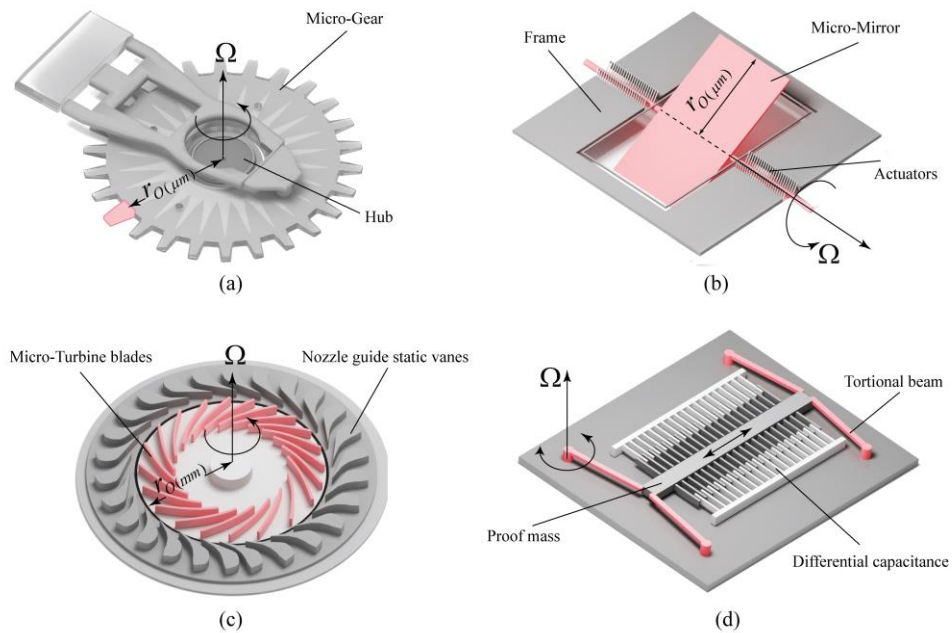


**Fig. 18** (a) Micro scale mechanical gear, (b)Micro-Mirror, (c) Micro-Turbine, (d) Micro scale accelerometer

**Acknowledgements:** *H.M. Sedighi is grateful to the Research Council of Shahid Chamran University of Ahvaz for its financial support (Grant No. SCU.EM99.98).*

## REFERENCES

1. Lord, H.W., Shulman, Y.H.,1967, *A generalized dynamical theory of thermoelasticity*, J. Mech. Phys. Solids,15(5), pp. 299–309.
2. Tzou, D.Y.,1992, *Thermal shock phenomena under high rate response in solids*, Annual Rev. Heat Transf., 4(4), pp. 111–185.
3. Tzou, D.Y.,1995, *A unified field approach for heat conduction from macro-to micro-scales*, J. Heat Transf., 117(1), pp. 8–16.
4. Tzou, D.Y.,1995, *The generalized lagging response in small-scale and high-rate heating*, Int. J. Heat Mass Transf., 38(17), pp. 3231–3240.
5. Abouelregal, A.E. 2019, *Two-temperature thermoelastic model without energy dissipation including higher order time-derivatives and two phase-lags*, Materials Research Express, 6(11), 116535.
6. Abouelregal, A.E.,2020, *On Green and Naghdithermoelasticity model without energy dissipation with higher order time differential and phase-lags*, Journal of Applied and Computational Mechanics, 6(3),pp. 445–56.
7. Abouelregal, A.E.,2019, *A novel generalized thermoelasticity with higher-order time-derivatives and three-phase lags*, Multidiscipline Modeling in Materials and Structures, doi: 10.1108/MMMS-07-2019-0138.
8. Abouelregal, A.E.,2019, *Three-phase-lag thermoelastic heat conduction model with higher-order time-fractional derivatives*, Indian J. Phys. <https://doi.org/10.1007/s12648-019-01635-z>.
9. Berman, R.,1953, *The thermal conductivity of dielectric solids at low temperatures*, Advances in Physics, 2(5), pp. 103-140.
10. Younis, M.I.,2011, *MEMS Linear and Non-linear Statics and Dynamics*, Springer, New York, USA.
11. Allameh, S.M.,2003, *An introduction to mechanical-properties-related issues in MEMS structures*, J. Mater. Sci., 38, pp. 4115–4123.
12. Sedighi, H.M., Bozorgmehri, A., 2016, *Dynamic instability analysis of doubly clamped cylindrical nanowires in the presence of Casimir attraction and surface effects using modified couple stress theory*,Acta Mech., 227, pp. 1575-1591.
13. Malikan, M., Uglov, N. S., Eremeyev, V.A., 2020,*On instabilities and post-buckling of piezomagnetic and flexomagnetic nanostructures*, International Journal of Engineering Science, 157, 103395.
14. Malikan, M., Eremeyev, V. A.,Žur, K. K.,2020,*Effect of Axial Porosities on Flexomagnetic Response of In-Plane Compressed Piezomagnetic Nanobeams*, Symmetry, 12(12), 1935.
15. Malikan, M., &Eremeyev, V.A., 2020,*On Nonlinear Bending Study of a Piezo-Flexomagnetic Nanobeam Based on an Analytical-Numerical Solution*, Nanomaterials, 10(9), 1762.
16. Malikan, M., Eremeyev, V.A., 2020,*On the Dynamics of a Visco-Piezo-Flexoelectric Nanobeam*, Symmetry, 12(4), 643.
17. Eringen,A.C.,1983, *On differential equations of nonlocal elasticity and solutions of screw dislocation and surface waves*, J Appl Phys, 54, pp. 4703–4710.
18. Eringen, A.C.,1972, *Nonlocal polar elastic continua*,Int J EngSci, 10, pp. 1–16.
19. Sedighi, H.M., Keivani, M., Abadyan, M.R., 2015, *Modified continuum model for stability analysis of asymmetric FGM double-sided NEMS: Corrections due to finite conductivity, surface energy and nonlocal effect*, Composites Part B: Engineering, 83, pp. 117-133.
20. Abouelregal, A.E., Marin, M.,2020, *The size-dependent thermoelastic vibrations of nanobeams subjected to harmonic excitation and rectified sine wave heating*, Mathematics; 8(7), 1128.
21. Barretta, R., Faghidian, S.A., Marotti de Sciarra, F., Pinnola, F.P., 2020, *Timoshenko nonlocal strain gradient nanobeams: variational consistency, exact solutions and carbon nanotube Young moduli*, Mechanics of Advanced Materials and Structures, 2020, doi: 10.1080/15376494.2019.1683660.
22. Abouelregal, A.E., Mohammed, W.W., 2020, *Effects of nonlocal thermoelasticity on nanoscale beams based on couple stress theory*, Mathematical Methods in the Applied Sciences, doi:10.1002/mma.6764.
23. Abouelregal A.E., Marin M.,2020, *The response of nanobeams with temperature-dependent properties using state-space method via modified couple stress theory*, Symmetry, 12(8), 1276.
24. Barretta, R., Faghidian, S.A., Marotti de Sciarra, F., Penna, R., Pinnola, F.P., 2020,*On torsion of nonlocal Lam strain gradient FG elastic beams*, Composite Structures, 233, 111550.
25. Shabani, S., Cunedioglu, Y. 2020, *Free vibration analysis of cracked functionally graded non-uniform beams*, Mater. Res. Express, 7, 015707.
26. Romano, G., Barretta, R., 2017, *Nonlocal elasticity in nanobeams: the stress-driven integral model*, International Journal of Engineering Science, 115, pp. 14–27.
27. Barretta, R., Feo, L., Luciano, R., Marotti de Sciarra, F., Penna, R., 2017, *Nano-beams under torsion: a stress-driven nonlocal approach*, PSU Research Review, 1(2), pp. 164-169.
28. Drexler, K. E., 1992, *Nanosystems: Molecular Machinery, Manufacturing, and Computation*, Wiley, New York, USA.

29. Han, J., Globus, A., Jaffe, R., Deardorff, G., 1997, *Molecular dynamics simulations of carbon nanotube-based gears*, Nanotechnology, 8, pp. 95–102.
30. Srivastava, D., 1997, *A phenomenological model of the rotation dynamics of carbon nanotube gears with laser electric fields*, Nanotechnology, 8, pp. 186–192.
31. Lohrasebi, A. Raffii-Tabar, H., 2008, *Computational modeling of an iondriven nanomotor*, J. Mol. Graphics Modell., 27, pp. 116–123.
32. Yokoyama, T., 1988, *Free vibration characteristics of rotating Timoshenko beams*, Int. J. Mech. Sci. 30, pp. 743–755.
33. Gunda J.B., Ganguli R., 2008, *New rational interpolation functions for finite element analysis of rotating beams*, Int. J. Mech. Sci., 50, 578–588.
34. Yoo, H.H., Park, J.H., Park J., 2001, *Vibration analysis of rotating pre-twisted blades*, Comput. Struct., 79(19), pp. 1811–1819.
35. Lee, S.Y., Lin, S.M., Lin, Y.S., 2009, *Instability and vibration of a rotating Timoshenko beam with precone*, Int. J. Mech. Sci. 51, pp. 114–121.
36. Avramov, K.V., Pierre, C., Shyriaieva, N., 2007, *Flexural-flexural-torsional nonlinear vibrations of pre-twisted rotating beams with asymmetric cross-sections*, J. Vib. Control., 13, pp. 329–364.
37. Mohammadi, M., Safarabadi, M., Rastgoo, A., Farajpour, A., 2016, *Hygro-mechanical vibration analysis of a rotating viscoelastic nanobeam embedded in a visco-Pasternak elastic medium and in a nonlinear thermal environment*, ActaMechanica, 227(8), pp. 2207–2232.
38. Faroughia, S., Rahmani, A., Friswell, M.I., 2020, *On wave propagation in two-dimensional functionally graded porous rotating nano-beams using a general nonlocal higher-order beam model*, Applied Mathematical Modelling, 80, pp. 169–190.
39. Ebrahimi, F., Haghi, P., 2017, *Wave propagation analysis of rotating thermoelastically-actuated nanobeams based on nonlocal strain gradient theory*, ActaMechanicaSolidaSinica, 30(6), pp. 647–657.
40. Azimi, M., Mirjavadi, S. S., Shafiei, N., Hamouda, A. M. S., Davari, E., 2017, *Vibration of rotating functionally graded Timoshenko nano-beams with nonlinear thermal distribution*, Mechanics of Advanced Materials and Structures, 25(6), pp. 467–480.
41. Narendar, S., Gopalakrishnan, S., 2011, *Nonlocal wave propagation in rotating nanotube*, Results in Physics, 1, pp. 17–25.
42. Ebrahimi, F., Dabbagh, A., 2018, *Wave dispersion characteristics of rotating heterogeneous magneto-electro-elastic nanobeams based on nonlocal strain gradient elasticity theory*, J. Electromag. Waves Appl., 32(2), pp. 138–169.
43. Noda, N., 1986, *Thermal stress in material with temperature dependent properties*, In: R.B. Hetnarski (Ed.), *Thermal stresses*, Elsevier Science, North Holland, Amsterdam, pp. 391–483.
44. Berman, R., 1953, *The thermal conductivity of dielectric solids at low temperatures*, Advances in Physics, 2(5), pp. 103–140.
45. Sharma, J.N., Kaur, R., 2015, *Response of anisotropic thermoelastic micro-beam resonators under dynamic loads*, Applied Mathematical Modelling, 39, pp. 2929–2941.
46. Honig, G., Hirdes, U., 1984, *A method for the numerical inversion of Laplace Transform*, J. Comp. Appl. Math., 10, 113–132.
47. Tzou, D.Y., 1995, *Experimental support for the lagging behavior in heat propagation*, J. Thermophys. Heat Transf. 9(4), pp. 686–693.
48. Wang, Y., Liu, D. Wang, Q., Zhou, J., 2016, *Asymptotic solutions for generalized thermoelasticity with variable thermal material properties*, Archives of Mechanics, 68(3), pp. 181–202.
49. Abo-Dahab, S.M., Abouelregal, A.E., Ahmad, H., 2020, *Fractional heat conduction model with phase lags for a half-space with thermal conductivity and temperature dependent*, Mathematical Methods in the Applied Sciences, doi:10.1002/mma.6614
50. Ebrahimi, F. Haghi, P. 2018, *Elastic wave dispersion modelling within rotating functionally graded nanobeams in thermal environment*, Advances in Nano Research, 6(3), pp. 201–217.
51. Shafiei, N., Kazemi, M., Ghadiri, M., 2016, *Comparison of modeling of the rotating tapered axially functionally graded Timoshenko and Euler–Bernoulli microbeams*, Physica E: Lowdimensional Systems and Nanostructures, 83, pp. 74–87.
52. Younesian, D., Esmailzadeh, E., 2011, *Vibration suppression of rotating beams using timevarying internal tensile force*, Journal of Sound and Vibration, 330(2), pp. 308–320.
53. Khaniki, H.B., 2018, *Vibration analysis of rotating nanobeam systems using Eringen's two-phase local/nonlocal model*, Physica E: Low-Dimensional Systems and Nanostructures, 99, pp. 310–319.
54. Safarabadi, M., Mohammadi, M., Farajpour, A., Goodarz, M., 2015, *Effect of Surface Energy on the Vibration Analysis of Rotating Nanobeam*, Journal of Solid Mechanics, 7(3) pp. 299–311.

55. Fang, J., Gu, J., Wang, H., 2018, *Size-dependent three-dimensional free vibration of rotating functionally graded microbeams based on a modified couple stress theory*, International Journal of Mechanical Sciences, 136, pp. 188-199.
56. Abouelregal, A.E. 2020, *A novel model of nonlocal thermoelasticity with time derivatives of higher order*, Mathematical Methods in the Applied Sciences, doi:10.1002/mma.6416.
57. Borjalilou, V., Asghari, M., Taati, E., 2020, *Thermoelastic damping in nonlocal nanobeams considering dual-phase-lagging effect*, Journal of Vibration and Control, 26(11–12), pp. 1042–1053.
58. Abouelregal, A.E., Zenkour, A.M., 2017, *Thermoelastic response of nanobeam resonators subjected to exponential decaying time varying load*, Journal of Theoretical and Applied Mechanics, 55(3), pp. 937-948, Warsaw.
59. Hahn, D.W., Özişik, M. N., 2012, *Heat conduction*, (3rd ed.), Hoboken, N.J., Wiley.